the stationary feature is very nearly the same as the meridional wave number of the alternating high-latitude jet streams, estimated as 2π divided by the peak-to-peak horizontal spacing of the eastward jets. Godfrey's (*1*) cloud-tracked wind measurements show peak eastward velocities at 76° and 61° north planetocentric latitude, corresponding to a meridional length scale for the jets of $L_J \approx 2.3 \times 10^6$ m $\approx r/6$. This coincidence may suggest that planetary wave number 6 is selected as the natural response to the same forcing that gives rise to the alternating zonal wind pattern. The inverse model analysis of the vertical structure problem for the inferred negative equivalent depth may therefore offer an important characterization of the planet's general circulation.

Further observational constraints on the deep atmospheric structure and dynamics of Saturn may be provided by a longwave (~ 10-cm) radiometry experiment on the Cassini orbiter. In the meantime, further interpretative studies of synoptic-scale features in the Voyager imaging data may offer the only observational avenue.

REFERENCES AND NOTES

1. D. A. Godfrey, *Icarus* **76**, 335 (1988).
2. ———, *Bull. Am. Astron. Soc.* **20**, 880 (1988). In this preliminary further study, the comparison of a Voyager 1 image taken 9 months before the Voyager 2 images analyzed in (*1*) implies a drift velocity for the hexagon of only just over 10 cm s^{-1}, less than the error in the corresponding drift of the measured SKR signal (*4*).
3. For precise navigation on an oblate planet it is important to distinguish between the planetocentric latitude λ_c, measured with respect to the planetary center, and the planetographic latitude λ_g, measured with respect to the vector normal to the local horizontal (equipotential) surface. The two are related as $\lambda_g = \tan^{-1}[(1-\epsilon)^{-2} \tan\lambda_c]$, where the planetary oblateness ϵ is the fractional difference between the equatorial and polar radii. To first order in the oblateness, the planetary radius varies with the planetocentric latitude as $a \approx a_e(1 - \epsilon \sin^2\lambda_c)$, where a_e is the equatorial value. For Saturn, $\epsilon \approx 0.098$ and $a_e = 60{,}270$ km. Although the observations are most directly navigated in the planetocentric system, the planetographic form is more directly related to the local normal projection of the planetary rotation, as required for dynamical analysis.
4. M. D. Desch and M. L. Kaiser, *Geophys. Res. Lett.* **8**, 253 (1981).
5. P. J. Gierasch, *Nature* **337**, 309 (1989).
6. M. Allison, D. A. Godfrey, R. F. Beebe, *Bull. Am. Astron. Soc.* **19**, 848 (1987).
7. J. Pedlosky, *Geophysical Fluid Dynamics* (Springer-Verlag, New York, ed. 2, 1987).
8. An excellent historical review of the observations, theory, and laboratory simulation of Rossby waves is given by G. W. Platzman, *Q. J. R. Meteorol. Soc.* **94**, 225 (1968).
9. M. Allison, *Icarus* **83**, 282 (1990).
10. L. A. Sromovsky, H. E. Revercomb, R. J. Krauss, V. E. Suomi, *J. Geophys. Res.* **88**, 8650 (1983).
11. The so-called potential vorticity is a conserved property of the motion, representing the balance of the total relative plus planetary vorticity in response to the vertical stretching of a stratified column of rotating fluid. The relative vorticity is just the curl of the horizontal motion field, whereas the planetary vorticity is given as $f = 2\Omega \sin\lambda_g$. The stretching contribution is related to the vertical motion and static stability (or potential temperature stratification). A complete account of the theory is given by Pedlosky (*7*).
12. P. D. Thompson, *J. Meteorol.* **5**, 166 (1948).
13. G. J. Haltiner and R. T. Williams, *Numerical Prediction and Dynamic Meteorology* (Wiley, New York, ed. 2, 1980).
14. J. G. Charney, in *Dynamic Meteorology*, P. Morel, Ed. (Reidel, New York, 1973), pp. 97–351.
15. P. J. Gierasch, *Icarus* **29**, 445 (1976).
16. According to the thermal wind shear analysis of Voyager infrared measurements by B. J. Conrath and J. A. Pirraglia [*Icarus* **53**, 286 (1983)], the vertical scale of variation of the cloud-top winds within the Saturn stratosphere amounts to about 6 pressure scale heights. The vertical shear below the cloud tops is essentially unconstrained by the available observations.
17. The given solution represents only the gravest wave mode satisfying the meridional structure prescribed by the adopted Gaussian jet profile. More generally, Eq. 3 assumes a form equivalent to the Schrödinger equation for the harmonic oscillator, with higher order solutions given by the Hermite polynomial functions. These higher order solutions have a broader meridional distribution, however, and probably exceed the latitudinal span of validity for the model representation of the ambient shear.
18. G. F. Lindal, D. N. Sweetnam, V. R. Eshleman, *Astron. J.* **90**, 1136 (1985).
19. I. M. Held, in *Large-Scale Dynamical Processes in the Atmosphere*, B. Hoskins and R. Pearce, Eds. (Academic Press, New York, 1983), p. 127–168.
20. R. S. Lindzen, *Q. J. R. Meteorol. Soc.* **94**, 402 (1968).
21. P. J. Gierasch and B. J. Conrath, in *Recent Advances in Planetary Meteorology*, G. Hunt, Ed. (Cambridge Univ. Press, Cambridge, 1985), pp. 121–146.
22. A. D. Del Genio and K. B. McGrattan, *Icarus*, in press.

11 September 1989; accepted 5 December 1989

The Strange Periodic Comet Machholz

DANIEL W. E. GREEN, HANS RICKMAN, ALAIN C. PORTER,* KAREN J. MEECH

The recently discovered periodic comet Machholz 1986 VIII (1986e) travels closer to the sun than any known planet and any known comet with an orbital period of less than 150 years, thus providing astronomers with a unique object for studying cometary evolution. The comet is spiraling steadily closer to the sun, from perihelion distance $q \simeq 0.9$ astronomical unit at about A.D. 700 to $q \simeq 0.13$ at present (orbital period, 5.25 years), to an expected $q \simeq 0.03$ by about 2450; should the comet survive such increasingly close perihelion passages, q will begin steadily to increase shortly thereafter. A review of observations made since discovery is presented, together with a discussion of numerical investigations of the comet's orbit over 4000 years and prospects for observing the upcoming return to perihelion in 1991.

A MOST UNUSUAL SHORT-PERIOD comet was discovered visually on 12 May 1986 by California amateur astronomer Donald Machholz (*1*), who was using a large pair of binoculars. Following the usual practice for a newly discovered comet, Marsden (*2*) computed parabolic orbital elements under the assumption that this object was traveling in a nearly parabolic, long-period (that is, orbital period >200 years) path around the sun, and he found that its orbit was also highly inclined ($i \sim 60°$) with respect to the ecliptic. Indeed, almost all comets discovered visually nowadays that have high-inclination orbits are long-period comets. As more observations became available, however, it soon became evident that this object has an orbital period (P) as short as 5.3 years, and hence it became known as periodic comet Machholz 1986 VIII = 1986e (hereafter, P/Machholz).

D. W. E. Green, Harvard-Smithsonian Center for Astrophysics, Cambridge, MA 02138.
H. Rickman, Astronomiska Observatoriet, 75120 Uppsala, Sweden.
A. C. Porter, California Institute of Technology, Pasadena, CA 91109.
K. J. Meech, Institute for Astronomy, University of Hawaii, Honolulu, HI 96822.

*Present address: Kitt Peak National Observatory, Tucson, AZ 85726.

What emerged as so unusual is the combination of the comet's short orbital period and high inclination, and its small perihelion distance ($q = 0.127$ AU). No other known comet with $P < 150$ years goes closer to the sun than P/Encke ($P = 3.3$, $q = 0.341$). Of the ~150 known short-period ($P < 200$ years) comets, only five have orbital periods less than that of P/Machholz (two of the five being considered "lost"). Most of these short-period comets belong to the so-called Jupiter family, characterized by relatively close approaches to Jupiter over periods of a few hundred years or less that affect the comets' orbits. P/Machholz apparently has not had such perturbing close approaches to Jupiter in thousands of years, even though its aphelion distance of $Q \simeq 5.9$ AU is well outside that planet's orbital distance ($a_J \simeq 5.2$ AU). P/Machholz's high orbital inclination is responsible for keeping the comet at a safe distance from Jupiter. Only four of the known periodic comets have orbits inclined more steeply (with respect to Earth's orbit) than does P/Machholz. The comet is in some respects similar to P/Halley-type comets, but such comets tend to have $P > 50$ years; it will be noteworthy if in the future other comets are found in orbits similar to that of P/Machholz.

How long can P/Machholz have been in such an orbit, and how much longer can it stay there, before (i) it is strongly perturbed by one or more major planets or (ii) it breaks apart from solar influences? P/Machholz's short orbital period should give astronomers a good opportunity to study the evolution of a comet from both physical and dynamical standpoints; the comet's proximity to the sun at perihelion suggests that changes in the state of P/Machholz's nucleus may be observable in only a few revolutions.

Green (*3*) discovered that the comet's perihelion distance has been slowly but steadily decreasing over the past few centuries. How P/Machholz's nucleus fares against increasingly closer trips to perihelion may give insight into the density and overall structure of the cometary nucleus. It is unclear whether such changes will be visible over a few apparitions, however, as a few revolutions may not be enough to change perceptibly the volatile content of the nucleus even at $q < 0.1$ unless the comet is already near the end of its resources; short-term variations in the nongravitational-force behavior of short-period comets appear to be influenced by varying amounts of dust coverage or nucleus precession, which changes the insolation conditions of the active spots (*4*). Changes in the nongravitational forces arising from such effects should be correlated with changes in the brightness behavior (either the absolute brightness level or the variation with time around each perihelion passage), but such changes are unfortunately much more difficult to ascertain. The smaller the perihelion distance, the slower would be the evolution of the dust coverage according to the simple idea of grains entailed by the outflowing gas up to a maximum size above which they remain on the surface (*5*). With the higher gas flux of small-q comets, grain accumulation would necessarily proceed more slowly. However, the actual situation may be much more complicated than this picture, and, in fact, an equally legitimate conjecture is that small-q comets usually have a long past history in short-period orbits so that extensive dust mantling of their nuclei may have occurred. It is interesting to compare P/Machholz to P/Encke and asteroid (3200) Phaethon, which may be cometary nuclei in small-q orbits that yet managed to develop dust coverage (*6*). As discussed below, there are indications that the nucleus of P/Machholz is active only over a low percentage of its surface, so in this sense it appears intermediate between P/Encke and (3200) Phaethon, if the latter is indeed an extinct comet.

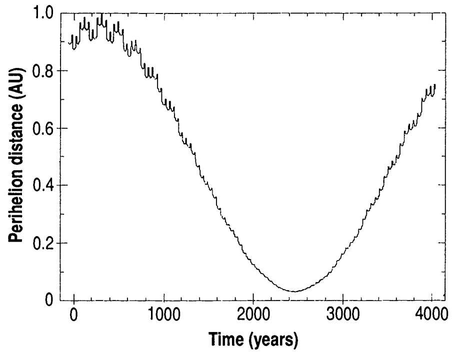

Fig. 1. Perihelion distance of P/Machholz as a function of time, given in years A.D. The wiggles appearing most clearly are caused by moderately close encounters with Jupiter occurring at intervals of ≈50 years. These are closest at both ends of the integration interval.

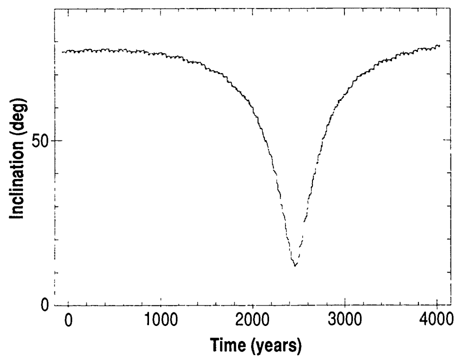

Fig. 2. Inclination of P/Machholz as a function of time, given in years A.D.

Integrating the orbit over many centuries is "risky" in that any small errors in the orbital elements or any close planetary encounters are magnified considerably as more integrating is performed. Nongravitational forces undoubtedly play a significant role on such a comet that passes so close to the sun at perihelion, but such forces cannot be reliably calculated until good astrometric observations covering at least three or four apparitions are available; even then they probably change with time. The present calculation indicates how and when an object, traveling in the given 1986 orbit, would encounter significant planetary perturbations and would give some insight into the time evolution of the orbital elements. The starting orbit is now fairly good, with 73 observations covering the period from 13 May 1986 to 6 April 1989 [mean residual, 0.9″ (*7*)].

Accurate orbital elements for 1986 are shown in Table 1. During the integrated interval of 548 years (1712 to 2260), no approach to Jupiter of <0.66 AU occurred. Four rather insignificant approaches (to within 0.1 AU) were found for Mercury (0.044 AU in 1722 and 0.056 AU in 1743), Venus (0.083 AU in 2250), and Earth (0.07 AU in 2229). We thus performed an extended integration to explore Jupiter's influence on the orbit of P/Machholz (*8*). The elliptic restricted three-body problem (sun-Jupiter-comet) was taken as the dynamical model (*9*), the integration interval being ≈2000 years backward and forward. Because of its high inclination, P/Machholz differs from the Jupiter family of comets, and by virtue of its Tisserand parameter ($J = 1.94$) it is more akin to short-period comets with $P > 20$ years (*10*), as far as its interactions with Jupiter are concerned. This means that encounters with the planet occur at high relative velocities, and, for a single such encounter to be efficient in changing the cometary orbit, it has to be very close. For a high-inclination orbit, such events can only occur when either of the nodes (that is, ecliptic plane crossings) is situated close to Jupiter's mean distance from the sun.

Table 1. Orbital elements of P/Machholz, epoch 1986 May 10.0 ET (ephemeris time). Listed below are the following oribtal elements: time of perihelion, T; eccentricity, e; perihelion distance, q; semimajor axis, a; argument of perihelion, ω; longitude of the ascending node, Ω; inclination, i [ω, Ω, and i are given for equinox 1950.0]; mean daily motion, $n°$; and orbital period, P.

Orbital element	Value
T	1986 April 23.51656 ET
e	0.9580123
q	0.1267741 AU
a	3.0193180 AU
ω	14.52644°
Ω	93.80578
i	59.98918
$n°$	0.18786280
P	5.246 years

It was therefore a surprise to see that, even in the absence of close encounters with Jupiter over ±2000 years (minimum distances, ≈0.5 to 0.6 AU), a major variation of the cometary orbit occurs. The Jovian perturbations occurring in the course of one orbital revolution are always weak, but they act in concert to produce a major exchange of angular momentum over a time scale of ~2000 years. Figures 1 and 2 illustrate how perihelion distance and inclination for this comet change over time. The angular momentum component perpendicular to the ecliptic is nearly conserved, as expected for this dynamical problem (*11*), but the in-plane component shows a drastic variation such that the perihelion point of P/Machholz appears to oscillate between Earth's orbit (1.0 AU) and the solar corona (~0.005 AU outward). The minimum perihelion distance is ≈0.03 AU and occurs in the 25th century; for comparison, q for Mercury is 0.31 AU. In connection with this, the inclination temporarily attains a value typical of the Jupiter family.

Figure 3 shows the evolution of the argument of perihelion (ω); a value near 0° or 180° means that the perihelion and aphelion points are situated near the ecliptic plane. Remarkably enough, ω varies monotonically but extremely slowly when near zero, so that the comet spends extended periods of time in an orbit with nearly 80° inclination, whose perihelion and aphelion points are near the orbits of Earth and Jupiter, respectively. The mean motion is quasi-stable, but interestingly the comet is close to the influential 2/1 resonance (the comet makes two revolutions in the same time that Jupiter makes one).

Figures 1, 2, and 3 suggest that the transfer of angular momentum is periodic and coupled to the variation of ω. Similar behavior was found by Froeschlé and Scholl (*12*) for fictitious high-inclination objects near the 2/1 resonance in connection with ω librations, so tentatively the mechanism operating on P/Machholz may be the same. Cometary orbital evolutions are generally chaotic as a result of close encounters with Jupiter (*10*), and the one shown in Figs. 1, 2, and 3 might well turn out to be chaotic, as well, if a longer time scale were considered, but this is as yet the single most dramatic orbital transformation of a comet found to occur in a quasi-regular pattern. The stability of the semimajor axis (Fig. 4) bears evidence of this and demonstrates that the comet keeps circulating on the inner side of the nearby 2/1 resonance during the whole integration interval. The longitude of perihelion stays near 100° all the time, so the longitude of the ascending node (Ω) varies approximately according to the scale indicated to the right in Fig. 3. We caution the reader that a simplified dynamical model has been used, where the nongravitational force was necessarily neglected. However, even if the actual comet might not follow in detail the evolution computed here, we certainly have a strong indication of a very peculiar dynamical behavior.

There has been much recent study concerning the evolution of cometary orbits as they are changed by planetary gravitational perturbations and by nongravitational forces (*13*). Investigators have speculated about the changes occurring in the materials of the cometary nucleus due to solar radiation effects received as a result of the comet's orbital motion (*14*). Over a period of repeated close approaches to the sun, those short-period comets that are not thrown out farther by planetary perturbations will eventually either disintegrate completely or evolve

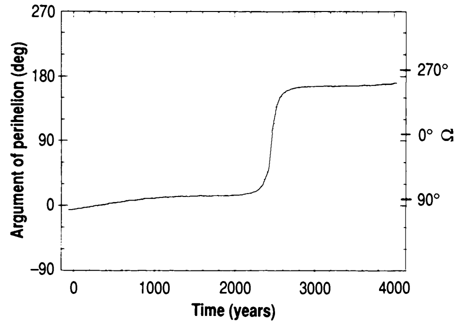

Fig. 3. Argument of perihelion (ω) as a function of time, given in years A.D. The actual variation of Ω differs from the one shown here by 10° at most, corresponding to the maximum variation of the perihelion longitude $\tilde{\omega} = \omega + \Omega$.

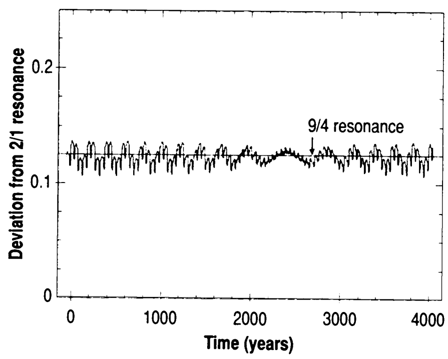

Fig. 4. The mean motion (n) is expressed as a fractional deviation $\delta(n) = (n - n_{res})/n_{res}$ from the value of the exact 2/1 resonance ($n_{res} = 2n_{Jup}$). The horizontal line marks the exact 9/4 resonance, which is, however, too weak to influence the large-scale evolution.

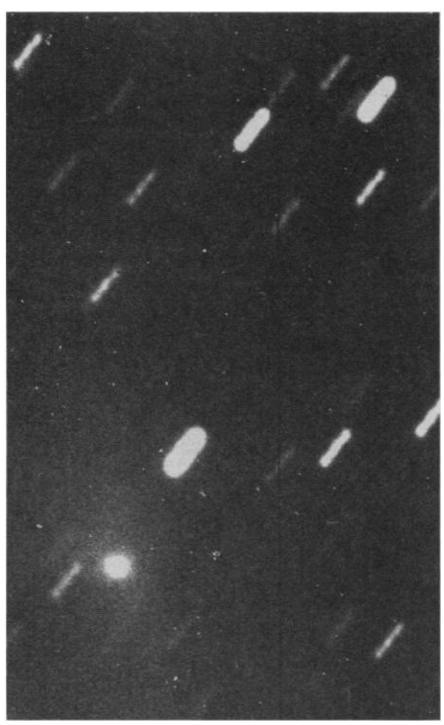

Fig. 5. CCD image of P/Machholz obtained on 1986 July 5.23 UT (360-s exposure with Gunn r filter; sec z = 1.16).

into inactive asteroidal-like objects as their volatile surface ices are depleted. Indeed, some asteroids are in unusual comet-like orbits (that is, high eccentricity), and a couple of short-period comets exhibit very little coma activity (implying that their nuclei are nearing an asteroid-like state). Asteroid (3200) Phaethon was the previous short-period record holder for perihelion distance; this unusual object, discovered in 1983, also travels in a comet-like orbit and is apparently connected with the Geminid meteor stream, traveling in essentially the same orbit (meteor streams have long been associated with comets). Indeed, it has been noted that P/Machholz may be related to the Quadrantid meteor stream (*15*), in particular since there is very good agreement of the longitudes of perihelia, and orbital evolutions like that of P/Machholz have been found for some Quadrantid meteors (*16*). There is a discrepancy in the nodes of P/Machholz and the Quadrantids, being nearly 180° apart, but the node of the comet appears to shift periodically between two opposite longitudes (Fig. 3). Further computations may reveal whether meteor particles can get out of phase with the comet in such shifts.

Since P/Machholz was already 3 weeks past perihelion when it was discovered in 1986, it gradually faded from total visual magnitude (m_1) 10 to 11 in mid-May to m_1 ~13 by late June. Photography and charge-coupled device (CCD) imaging indicate that the comet continued to fade to m_1 ~19.5 by early September, when it was last detected. Some 40 visual m_1 estimates of P/Machholz 1986 VIII made by ten observers have been published in the *International Comet Quarterly* (*17*). The total visual magnitude of a comet represents the total integrated brightness of the visible coma and is a good indication of cometary activity (*18*); a representative power-law formula is

$$m_1 = 13.0 + 5 \log \Delta + 12 \log r \qquad (1)$$

where Δ and r are the comet's geocentric and heliocentric distances, respectively. Equation 1 provides a fairly good fit for postperihelion observations in the range 0.66 AU < r < 2.48 AU. (Use caution when applying this equation to preperihelion observations in 1991, since comets typically have asymmetric light curves with respect to perihelion.)

The comet displayed a faint, tenuous coma (diameter up to 4′ to 5′) with a fairly strong central condensation in May and June 1986, and short tails, pointing both toward and away from the sun, were noted by observers (*17*). Short-focus telescopes revealed a much larger coma than did long-focus instruments.

CCD images of P/Machholz were obtained (by A.C.P.) with the 1.5-m (60-inch) reflector at Palomar Observatory (*19*) on 5, 6, 7, and 8 July 1986 UT, when the comet was at $\Delta \simeq 0.8$ AU and $r \simeq 1.7$ AU. Images were taken in the Thuan-Gunn r passband (*20*) on all four nights, and in the g, i, and z bands of that system on some of the other nights. The series of g and r pictures show a strong evolution in the compactness of the comet. A strong central condensation ("false" nucleus) was visible on all four nights. On 5 July, it was surrounded by a large, faint, elliptical coma, which filled most of the field of view, and there was a distinct fan-shaped tail extending to the northeast (Fig. 5). The opening angle of the tail is close to 60° with a relatively sharp edge in position angle 11°. A faint jet was also visible extending southward. On 6 July, the coma and tail were still visible but were noticeably fainter and featureless. On 7 July, only a faint, stubby tail was left, and the images taken on 8 July were nearly stellar. On 5 July, a relatively sharp boundary between the nucleus and coma occurred 6″ from the center of the comet, 3 mag/arc sec^2 below the central surface brightness. On 6 July, the onset of the coma occurred 4 mag/arc sec^2 below and 5″ from the nucleus. No surface brightness profile was measured for 7 July, because the comet was superposed on a bright star. On 8 July, the comet was almost completely stellar. The coma appeared 4.5 mag/arc sec^2 below the central surface brightness, a level that is reached at a radius of only 3″.

It is thus clear that a significant change in the morphology of the comet took place between 5 and 8 July. The shrinkage of its nucleus and the fading of its coma indicate that outgassing from the nucleus either stopped or was drastically reduced shortly before the pictures were taken. The observed shallowness of the surface brightness profile is consistent with this hypothesis, for it could be a consequence of the depletion of the denser inner regions of the coma before its outskirts. The quality of the images is not good enough to permit us to date the turnoff, but it probably did not occur much before 3 July.

Large reflectors can detect P/Machholz throughout its orbit, as proven by the recent observations that were made while the comet was relatively near aphelion in early December 1988. On 6.3 April 1989 UT, Meech found $m_2 = 22.5$ with the 1.5-m f/7.5 reflector (+ Mould R filter + CCD) at Cerro Tololo Interamerican Observatory. Further observations on 3 June 1989 yielded $m_2 = 21.8$ (Mould R). The 1988–1989 measurements of P/Machholz (when its appearance was stellar) (*21*) suggest the following "nuclear" magnitude formula:

$$m_2 = 14.5 + 5 \log \Delta + 5 \log r \qquad (2)$$

This is not much more than one magnitude fainter than the P/Halley nucleus, a finding that contrasts sharply with the very faint total magnitude from Eq. 1. Thus we have a clear indication that the nucleus of P/Machholz is in a state of very low activity, outgassing from less than 1% of the surface (*22*).

Why was P/Machholz not discovered before 1986? Once every several revolutions or so, the comet comes within ~0.5 AU of Earth, as it did in June 1986 ($\Delta = 0.40$ AU), May–June 1965, and May–June 1944. We calculated ephemerides for each return of P/Machholz to perihelion from 1928 to 1981, using Eq. 1 as a guide to the comet's brightness. This reveals that the comet is usually at very small solar elongations (<30° to 40°) when it is brighter than $m_1 \sim 11$ and that it is not usually brighter than $m_1 \sim 17$ when near opposition. Also, before perihelion P/Machholz is very far south (declination usually < −40° for elongation >40°), precluding potential for discovery from the Northern Hemisphere (where there have always been many more observers). Observers with large-field (for example, Schmidt telescopes and astrographs) photographs going to limiting stellar magnitude 19 or fainter are urged to check whether plates are available covering the following coordinates (right ascension, α, and declination, δ, given for equinox 1950.0) and times, which are near the comet's perihelia: May–June 1981 ($\alpha \sim 19^h$, $\delta \sim -12°$), June–July 1975 ($\alpha \sim 23^h$, $\delta \sim -60°$ to $-70°$), June–July 1965 ($\alpha \sim 19^h$ to 16^h, $\delta \sim +25°$ to $-5°$), June–July 1954 ($\alpha \sim 23^h$, $\delta \sim -60°$ to $-70°$), and June–July 1944 ($\alpha = 18^h$ to 16^h, $\delta = +50°$ to $+5°$). If such plates are available, the first author (D.W.E.G.) can supply better search ephemerides. A search by R. H. McNaught of Schmidt plates at Siding Spring Observatory has yielded nothing.

Some researchers have found that observations of comets previously recorded as minor planets were, in fact, prediscovery observations of short-period comets (*23*). With this in mind, Green (*3*) searched for such possible observations back to the turn of the 20th century, with no success.

Comets do occasionally break apart, some apparently reaching extinction (*14*). It is unknown how P/Machholz will "perform" as it gradually "spirals" toward the sun, but it is thus far a unique object among known comets. For this reason, astronomers should give the highest priority to observations of P/Machholz around the time of perihelion in 1991 and at subsequent apparitions. Of particular use will be observations yielding accurate astrometry (for improvement of the orbit), V photometry, spectrophotometry, and spectroscopy.

The comet will be within 30° elongation from the sun during the period from 10 July to 5 August 1991 (time of perihelion = 22 July 1991). For a month or so before that, Southern Hemisphere observers may be able to follow the comet while it is around $m_1 \simeq 11$ to 13; for a month or so after 5 August, Northern Hemisphere observers should have a similar opportunity.

REFERENCES AND NOTES

1. D. E. Machholz, *Int. Astron. Union Circ. 4214* (Central Bureau for Astronomical Telegrams, Smithsonian Astrophysical Observatory, Cambridge, MA, 1986).
2. B. G. Marsden, *Int. Astron. Union Circ. 4217* (1986).
3. D. W. E. Green, *Int. Comet Q.* **8**, 110 (1986); the integration was later extended to the period 1712 to 2260.
4. The influence of varying dust coverage was tentatively inferred by H. Rickman, M. C. Festou, L. Kamél, and C. Froeschlé [in *Diversity and Similarity of Comets*, E. J. Rolfe and B. Battrick, Eds. (ESA Publication SP-278) (European Space Agency, Noordwijk, The Netherlands, 1987), p. 471]. Changing insolation conditions on a nucleus with a precessing spin axis were introduced as an essential feature in the modeling of P/Encke's nongravitational-force behavior by F. L. Whipple and Z. Sekanina [*Astron. J.* **84**, 1894 (1979)].
5. F. L. Whipple, *Astrophys. J.* **111**, 375 (1950). For a review of more recent developments, see T. I. Gombosi, A. F. Nagy, T. E. Cravens, *Rev. Geophys.* **24**, 667 (1986).
6. Arguments that the nucleus of P/Encke is extensively dust-covered were given by: D. Jewitt and K. Meech, *Astron. J.* **93**, 1542 (1987); H. Rickman, in *Interplanetary Matter*, Z. Ceplecha and P. Pecina, Eds. *Publ. Astron. Inst. Czech. Acad. Sci. No. 67*, vol. 2, p. 37 (1987); Z. Sekanina, *Astron. J.* **95**, 911 (1988). The asteroid (3200) Phaethon is associated with the Geminid meteor stream, and this association is more easily explained in terms of past cometary activity than in terms of asteroidal collisions [see J. Hunt, K. Fox, I. P. Williams, in *Asteroids, Comets, Meteors II*, C.-I. Lagerkvist, B. A. Lindblad, H. Lundstedt, H. Rickman, Eds. (Uppsala University, Uppsala, Sweden, 1986), p. 549; G. W. Wetherill, *Icarus* **76**, 1 (1988)].
7. Orbital elements for epoch 1991, covering observations from 1986 to 1989, were published by D. W. E. Green, *Minor Planet Circ. 14748* (1989) (Minor Planet Center, Smithsonian Astrophysical Observatory, Cambridge, MA). The available astrometric observations of P/Machholz are in *Minor Planet Circ. 10676, 10677, 10794, 10795, 10893, 10998, 11111, 14669*, and *14670*. Some 40 observations with residuals >2.5″ were not used herein.
8. The starting orbit used for the long integrations is that published in *Minor Planet Circ. 11153*, spanning the arc 13 May 1986 to 5 September 1986; the orbital elements are very similar to those in Table 1.
9. The integration program is based on the one used by Cl. Froeschlé and H. Rickman [*Astron. Astrophys.* **82**, 183 (1980)] and uses a Bulirsch-Stoer integration of equations of motion regularized according to the Kustaanheimo-Stiefel and Birkhoff transformations.
10. The Tisserand parameter [F. Tisserand, *Traité de Mécanique Céleste*, tome IV (Gauthier-Villars, Paris, 1896)] is a simple function of orbital elements approximating the Jacobi integral, which gives the specific energy of the comet in a frame rotating with the orbital motion of Jupiter (assumed circular). It directly relates to the speed of encounter with Jupiter [E. J. Öpik, *Adv. Astron. Astrophys.* **2**, 219 (1963)] and provides a useful criterion for dynamical classification of short-period comets [A. Carusi and G. B. Valsecchi, in *Interplanetary Matter*, Z.

Ceplecha and P. Pecina, Eds. *Publ. Astron. Inst. Czech. Acad. Sci. No. 67*, vol. 2, p. 21 (1987); H. Rickman and Cl. Froeschlé, *Celestial Mech.* **43**, 243 (1988)].
11. This is a well-known result that comes from the quasi-conservation of the Tisserand parameter and the quasi-constancy of the semimajor axis in the absence of close encounters with Jupiter. Mathematically, this leads to: $\sqrt{a(1-e^2)} \cos i \approx$ const.
12. Cl. Froeschlé and H. Scholl, *Astron. Astrophys.* **111**, 346 (1982).
13. See A. Carusi and G. B. Valsecchi, Eds., *Dynamics of Comets: Their Origin and Evolution* (Reidel, Dordrecht, 1985).
14. Z. Sekanina discusses the distintegration of comets in *Icarus* **58**, 81 (1984) and the splitting of comets in *Comets*, L. Wilkening, Ed. (Univ. of Arizona Press, Tucson, 1982), pp. 251–287. See also the papers by L. Kresák (and references therein): in (*13*), p. 279; *Int. Comet Q.* **9**, 59 (1987).
15. B. McIntosh, paper presented at the "Comets in the Post-Halley Era" conference, Bamberg, West Germany, April 1989.
16. S. E. Hamid and M. N. Youssef, *Smithsonian Contrib. Astrophys.* 7, 309 (1963).
17. D. W. E. Green, Ed., *Int. Comet Q.* **8**, 43 (1986); *ibid.*, p. 46; *ibid.*, p. 85; *ibid.*, p. 89; *ibid.* **9**, 80 (1987).
18. ———, T. L. Rokoske, C. S. Morris, in *Proceedings of the 20th ESLAB Symposium on the Exploration of Halley's Comet*, B. E. Battrick, E. J. Rolfe, R. Reinhard, Eds. (ESA Publication SP-250) (European Space Agency, Noordwijk, The Netherlands, 1986), vol. 3, pp. 249–251. See also D. W. E. Green and C. S. Morris, *Astron. Astrophys.* **187**, 560 (1987).
19. The detector used was an RCA 512×320 chip with 27-μm pixels. At the *f*/8.75 Cassegrain focus, this gives an image scale of 0.46" per pixel, and a field of view of 4′ × 2.5′. The telescope was tracked to follow the motion of the comet. Most exposures were 6 or 10 min long. Absolute photometry of the images is, unfortunately, not possible, since of the four nights, only 7 July was photometric, and, on that night, only one image was taken, in which the comet overlapped a bright star trail.
20. T. X. Thuan and J. E. Gunn, *Publ. Astron. Soc. Pac.* **88**, 543 (1976).
21. G. Pizarro, O. Pizarro, R. M. West, *Minor Planet Circ. 14669* (1989). K. J. Meech, *Minor Planet Circ. 14670* (1989); magnitudes of comparison stars from A. U. Landolt, *Astron. J.* **78**, 959 (1973).
22. This is also commented upon by Z. Sekanina, *Astron. J.*, in press.
23. S. Nakano, *Minor Planet Circ. 8694* and *8695* (1984), *12025* (1987), and *12626* (1988); 16 cases of comets that were originally given minor planet designations are listed by B. G. Marsden, in *Catalogue of Discoveries and Identifications of Minor Planets* (International Astronomical Union Minor Planet Center, Smithsonian Astrophysical Observatory, Cambridge, MA, ed. 2, 1986), p. 140.
24. Useful discussions were provided by B. G. Marsden, C. M. Bardwell, and Z. Sekanina. We thank J. Briggs and the late E. Everhart, Chamberlin Observatory, University of Denver, and J. V. Scotti and T. Gehrels, Lunar and Planetary Laboratory, University of Arizona, for looking at astrometric data in search of more photometric information. We thank R. H. McNaught, Siding Spring Observatory, for searching old plates for possible images of P/Machholz. A.C.P.'s research at Caltech was supported in part by an ARCS fellowship.

14 September 1989; accepted 29 November 1989

Interparticle Collisions Driven by Ultrasound

Stephen J. Doktycz and Kenneth S. Suslick*

Ultrasound has become an important synthetic tool in liquid-solid chemical reactions, but the origins of the observed enhancements remained unknown. The effects of high-intensity ultrasound on solid-liquid slurries were examined. Turbulent flow and shock waves produced by acoustic cavitation were found to drive metal particles together at sufficiently high velocities to induce melting upon collision. A series of transition-metal powders were used to probe the maximum temperatures and speeds reached during such interparticle collisions. Metal particles that were irradiated in hydrocarbon liquids with ultrasound underwent collisions at roughly half the speed of sound and generated localized effective temperatures between 2600°C and 3400°C at the point of impact for particles with an average diameter of ~10 μm.

The chemical effects of high-intensity ultrasound result primarily from acoustic cavitation: the formation, growth, and implosive collapse of bubbles in liquids (*1–5*). In heterogeneous, solid-liquid reactions, ultrasound has increased the reactivity of metal powders by as much as 100,000-fold (*6*). Ultrasound has become an important tool in chemical synthesis involving mixed-phase reactions (*1–3, 7–9*). Studies on the effect of ultrasound on metal powders have shown dramatic changes in particle morphology, substantial agglomeration of powders, and significant reduction of passivating surface oxide coatings (*6, 10–15*). Still the origins of the dramatic enhancements observed with heterogeneous sonochemistry have remained unclear.

Acoustic cavitation in liquids generates implosive bubble collapse and associated shock waves. Bubble collapse near an extended surface can also produce localized, high-speed jets of liquid that impinge on the surface (*16–19*). Fine powders, however, are too small to perturb the ultrasonic field. At 20 kHz, for example, simple calculations indicate that the collapsing bubble will have a diameter of ~150 μm (*1, 19*); solid particles smaller than this size cannot cause microjet formation. In the presence of small particles, however, normal cavitational collapse will still occur.

The shock waves so generated can cause small particles to collide into one another with great force, producing interparticle melting, as illustrated in Fig. 1 for a Zn powder with an average diameter of 5 μm. The two Zn particles, originally separate spheres, are fused together after impact. The formation of a neck of Zn metal joining the two particles can be seen in the scanning electron micrograph. We believe that this neck originates from the rapid cooling of the effectively molten collision zone as the colliding particles rebound immediately after impact.

The Sn [<44 μm average diameter, mp (melting point) 232°C] and Fe (5 μm average diameter, mp 1535°C) particles were ultrasonically irradiated for 30 min in decane, which resulted in fusion of the different metal particles (Fig. 2). As in the case of the Zn particles, a melted neck joins the two particles. A scanning Auger electron spectroscopy dot map of elemental Sn shows that the Sn particle and the melted neck area to be made mainly of Sn, as expected from the relative melting points of the metals.

In order to determine roughly the maxi-

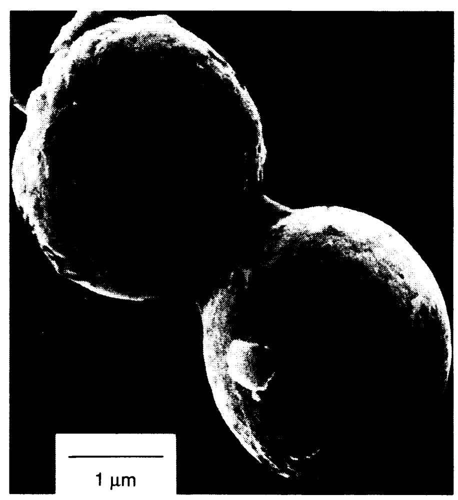

Fig. 1. Scanning electron micrograph of 5-μm average diameter Zn powder. Neck formation from localized melting is caused by high-velocity collisions. The metal powders (Mallinckrodt) were irradiated 30 min at 15°C in freshly distilled decane (17 ml, ~20% by weight) under Ar, with direct-immersion ultrasonic horn (Heat Systems) at 20 kHz and 50 W/cm². The slurry was then filtered, washed with pentane, and dried under vacuum at ~75°C for 24 hours. Scanning electron micrographs were taken on a Hitachi S-800 at 20-kV accelerating voltage.

School of Chemical Sciences, University of Illinois at Urbana-Champaign, Urbana, IL 61801.

*To whom correspondence should be addressed.